RSC Advances

PAPER

View Article Online
View Journal | View Issue

Cite this: *RSC Adv.*, 2023, **13**, 1906

Catalytic ozonation of sulfamethoxazole using low-cost natural silicate ore supported Fe_2O_3: influencing factors, reaction mechanisms and degradation pathways†

Lisha Luo, [ab] Zhiyu Sun,[b] Yuxi Chen,[a] Hui Zhang,[b] Yinkun Sun,[b] Dongwei Lu *[b] and Jun Ma [b]

Received 24th October 2022
Accepted 17th December 2022

DOI: 10.1039/d2ra06714e

rsc.li/rsc-advances

A low-cost natural silicate ore supported Fe_2O_3 (FeSO) was synthesized for catalytic ozonation of sulfamethoxazole (SMX). XRD, SEM-EDS, BET, FTIR and XPS results of the FeSO catalyst confirmed that the natural silicate ore was successfully modified with iron oxide. The effects of key factors, such as catalyst dosage, initial solution pH, reaction temperature, inorganic anions and initial concentration, on ozonation degradation were systemically investigated. The degradation rate of SMX (20 mg L^{-1}) was 88.1% after 30 min, compared with only 35.1% SMX degradation rate in the absence of the catalyst, and the total organic carbon (TOC) removal reached 49.1% after 60 min. Reaction mechanisms revealed that surface hydroxyl groups of FeSO were a critical factor for hydroxyl radical (•OH) production leading to fast SMX degradation in the ozone decomposition process. The degradation products were detected, and the possible pathways of SMX were then proposed. This study provides guidance for preparing a low-cost catalyst and analyzing the degradation products and pathways of SMX in the ozonation process, which is of significance in practical industrial applications.

1. Introduction

Sulfamethoxazole (SMX) is a synthetic antimicrobial that is used worldwide as a medicine for the prevention and treatment of infections, as well as in feed additives.[1] The frequent detection of SMX in natural aquatic environments has prompted growing public concern due to its potential risks to the ecosystem and humans, even at trace concentrations.[2] SMX has been repeatedly detected at concentrations as high as 24.8 μg L^{-1} in wastewater treatment plant (WWTP) secondary effluent and 940 ng L^{-1} in surface water.[3] Moreover, the traditional sewage biological treatment technology (STP) cannot effectively remove sulfonamide antibiotics due to its poor biodegradability.[4] These pollutants can end up in the receiving waters and even in drinking water.[5] The discharge standard of SMX for mariculture wastewater is lower than 0.02 μg L^{-1} (DB 21/T 2428-2015). Therefore, it is of great significance to exploit effective technologies to degrade SMX in aqueous solution.

Advanced Oxidation Process (AOPs) is based on the generation of highly active species, such as hydroxyl radical (•OH, redox potential = 2.80 V), which can rapidly remove the organic pollutants in water. Currently, it has been successfully applied to remove SMX.[6–10] Typical advanced oxidation technologies include wet catalytic oxidation,[7] electrochemical oxidation,[8] photocatalytic oxidation[9] and Fenton methods,[10] as well as rapidly developing ozone catalytic technologies.[11] The residual problem of H_2O_2, the solid–liquid separation problem of nano photocatalyst, the cost and practicability of UV lamp have seriously affected the application of AOPs in the actual wastewater treatment process. Ozone as a kind of strong oxidizer (2.07 V) has the powerful oxidation ability for the organic pollutants. It can degrade the organic pollutants by two pathways of the direct oxidation by ozone molecules and indirect oxidation of the reactive oxygen species generated by ozone during organics decomposition process.[12] Compared to homogeneous catalytic ozonization, the solid catalyst of heterogeneous catalytic ozonization can adsorb organics on the catalyst surface to accelerate the subsequent reaction between pollutant and ozone. This process can improve the utilization rate of ozone and enhance decomposition of ozone to product more hydroxyl radicals.[7] Moreover, the solid catalysts for heterogeneous catalytic ozonization are easily separated from aqueous and reused, and thus have overall lower-cost.[13,14]

Several types of catalysts have been widely used such as metal oxides (TiO_2, CeO_2 and Fe_2O_3), natural and artificial minerals (zeolites and honeycomb), carbonaceous matters (carbon

[a]Jilin Institute of Chemical Technology, Jilin 130022, P. R. China
[b]State Key Laboratory of Urban Water Resource and Environment, Harbin Institute of Technology, Harbin 150090, PR China. E-mail: lvdongwei@hit.edu.cn

† Electronic supplementary information (ESI) available. See DOI: https://doi.org/10.1039/d2ra06714e

nanotubes and activated carbon) and metal supported compounds (metal supported minerals or metal oxides) for catalytic ozonation application.[15–17] Recently, Fe-based metal oxidation catalysts have received more attention due to the high oxygen storage capacity, easy synthesis and non-toxic and abundant in nature.[18] In addition, some porous materials of carbon based material, molecular sieve, honeycomb ceramics have been used as supporters in order to improve the stability or the specific surface area of catalysts.[19–21] Compared to the artificial materials, the natural silicate ore is relatively cheap, innocuous, eco-friendly and more accessible, thus an ideal support for Fe-based metal oxidation catalysts.[22–25] Moreover, it has the advantages of developed pore structure, high specific surface area and perfect reusability according to our previous work.[7,26] Overall, natural silicate ore supported Fe_2O_3 (FeSO) could be a low-cost and efficient catalyst. However, the catalytic performance of the iron modified silicate ore (FeSO) in ozonation process of SMX has not been reported, and its influencing factors, catalytic mechanisms and degradation pathways still remain unrevealed.

In this work, natural silicate ore supported Fe_2O_3 (FeSO) has been successfully synthesized for catalytic ozonation of SMX as the model refractory micropollutant. The key factors during catalytic process and catalyst stability were investigated in the catalytic ozonation system. Moreover, the degradation intermediates were detected and the possible pathways of SMX were proposed for better guiding the real application of the catalytic ozonation of FeSO system.

2. Materials and methods

2.1 Materials and instruments

Silicate ore were obtained from Heilongjiang province. $Fe(NO_3)_3 \cdot 9H_2O$ and *tert*-butyl alcohol (TBA) were purchased from Sinopharm Chemical Reagent Co. Ltd (Shanghai, China). SMX was purchased from Tokyo Chemical Industry Co., Ltd (Tokyo, Japan). Sodium hydroxide, sodium hydrogen sulfite, sodium bicarbonate, sodium phosphate, benzoic acid, hydroxybenzoic acid, and hydrochloric acid were from Tianjin Damao Chemical Agent Factory (Tianjin, China). Methanol and acetic acid were of HPLC grade. Deionized water (18 MΩ cm) was used for the experiments. The pH value of the solution was adjusted with diluted HCl and NaOH. The information of instruments was present in the ESI (Table S1†).

2.2 Preparation and characterization of FeSO catalyst

The mesoporous catalyst FeSO was prepared by impregnating iron metal into silicate ore (SO) using wetness impregnation method. The natural SO particles were firstly washed and grinded. Ferric nitrate ($Fe(NO_3)_3 \cdot 9H_2O$) of 0.5 mol L^{-1} as precursor, was dissolved in deionized water of 100 mL, and then SO of 5.0 g was added to the above solution. The mixture was stirred for 24 h, followed by filtration and dried in an oven at 105 °C overnight. It was finally calcined at 500 °C for 4 h to obtain a FeSO catalyst.

The morphology and element distribution of the obtained sample were characterized by scanning electron microscope (SEM) and energy dispersive X-ray detector (EDS). X-ray powder diffraction (XRD) analysis was carried out using a XRD instrument. The N_2 adsorption–desorption isotherms were attained at 77 K on a Quantasorb surface area analyzer. The pore size distribution, pore volume, and average pore diameter were determined by the Barrett–Joyner–Halenda (BJH) and Brunauer–Emmett–Teller (BET) methods. The element contents of FeSO and SO were determined by X-ray photoelectron spectroscopy (XPS).

2.3 Catalytic ozonation procedure

The experimental set up for catalytic ozonation process was carried out with a semi-batch mode. Ozone was generated from pure oxygen by a 3S-A5 ozone generator (Tonglin Technology, Beijing), and then the ozone was continuously fed into a 0.5 L aqueous solution containing SMX at a flow rate of 200 mL min^{-1}. Usually, ozone concentration was 0.4 mg min^{-1}, catalyst dosage was 1.0 g L^{-1} and SMX concentration was 20 mg L^{-1}, respectively. The solution was stirred by a magnetic stirrer. The reaction temperature kept at 293 ± 1 K. The initial pH of the solution was about 7.

2.4 Analytical method

The samples were withdrawn through cellulose acetate filters (pore size 0.22 μm) for analysis at given time intervals, and the reaction was quenched by 0.1 M $Na_2S_2O_3$ solution. The SMX concentration was determined using an High Performance Liquid Chromatography (HPLC) (277 nm) (Zorbax extend-C18 column (5 μm × 4.6 mm × 150 mm), 0.8 mL min^{-1} flow, and mobile phase methanol/acetic acid (1‰) (90/10 in v/v)). A Shimadzu TOC 5000 analyzer was used to measure total organic carbon (TOC). The dissolved ozone concentration in the aqueous phase was measured by the indigo method.[14] The gas ozone concentration was measured by the iodometric method.[15] The released iron ions from the catalysts in the reaction process were measured using inductively coupled plasma (ICP) (PerkinElmer Optima 5300DV). Fluorescence spectra were investigated using a FP-6500 fluorescence spectrophotometer (JASCO, Japan) at an excitation wavelength of 303 nm. The solution pH was determined by a PHS-3C pH meter (Leici). The oxidation intermediates of SMX were detected by a Liquid Chromatography/Mass spectroscopy (LC/MS) with an electrospray ionization (ESI) source (HPLC/ESIQqQMS, Agilent 1260 HPLC-ABSciex QTrap 5500 MS) in positive ion mode. Sample separation was carried out with a C18 column (Waters XBridge, 3.0 × 100 mm, 2.5 μm particle size) at a flow rate of 0.2 mL min^{-1}. The injection volume of sample was 10 μL, and acetonitrile and ultrapure water (containing 0.1% formic acid) were used as the mobile phase. Gradient mobile phase was shown on Table S2.† Operating parameters of MS were operated as follows: full-scan mode; mass spectra scan range, 40–500 Da; ion spray voltage, 5500 V; source temperature, 550 °C; curtain gas, 35 arbitrary units; ion source gas I, 50 arbitrary units; ion source gas II, 50 arbitrary units; declustering potential, 90 V; collision cell exit potential, 18 V; entrance potential, 10 V.

3. Results and discussion

3.1 Characterization of catalysts

3.1.1. Morphology. The SEM images and EDS spectra of SO and FeSO were exhibited in Fig. 1. As shown in Fig. 1a and b, the natural silicate ores were mainly small debris. After the modification (Fig. 1c and d), the FeSO showed the smoother surface, and the small clumps of SO agglomerated together to form larger one due to the calcination. Fig. 1e and f provided the EDS spectra of SO and FeSO samples. The element peaks of Si, Al, O were found in natural silicate ore. Moreover, peaks of Fe elements (24.5%) were observed from the EDS spectrum of FeSO, which proved the successful loading of iron oxide on the surface of SO (the loading rate of Fe_2O_3 on SO was about 35%). Fig. 1g–j showed the EDS mapping images of FeSO, in which the iron element was uniformly distributed. The formation of iron oxides and their evenly distribution play an important role for catalytic ozonization of refractory organic pollutants.[26]

3.1.2. Crystallographic structure. The XRD patterns of SO and FeSO were shown in Fig. 1k. The natural SO sample exhibited the strong diffraction peaks at 2θ values of 21.8 (111), 35.9 (220) and 26.6 (011), which were well associated with the characteristic peaks of cristobalite (JCPDS no. 89-3607) and a-quartz (JCPDS no. 85-1054).[25] In contrast, several peaks of 24.1°, 33.2°, 35.7°, 40.9°,49.5°, 54.1°, 62.5° and 64.0° for α-Fe_2O_3 (JCPDS no. 73-2234) appeared in FeSO.[27] The characteristic diffraction peaks of SO in FeSO showed a lower intensity compared with the natural SO. The XRD results again concluded that the Fe_2O_3 was effectively.

3.1.3. BET surface area and pore size distributions. The surface areas, pore volumes and diameters of SO and FeSO samples were characterized by N_2 adsorption–desorption. As shown in Table S3,† the surface areas of SO and FeSO were 69.04 $m^2\ g^{-1}$ and 53.50 $m^2\ g^{-1}$, respectively. The results showed that the surface area, pore volume and size of FeSO decreased after loading of iron. This is because that the Fe_2O_3 dispersed and partially blocked into the SO pores. The specific surface area and characteristic porosity of tourmaline were investigated by N_2 adsorption/desorption measurements shown in Fig. 1i.

According to IUPAC classification, the isotherm of the SO and FeSO exhibited a type IV pattern with a type H3 hysteresis loop, indicating the presence of mesopores.[28]

3.1.4. Surface composition and chemical state. The elements in SO and FeSO were also determined by XPS in Fig. 2a. Compared with the full-scale spectrum of SO, Fe element peaks were detected in FeSO, confirming the presence of Fe in the FeSO composites. The O 1s region could be decomposed into four peaks (Fig. 2b). The peak located at 529.8 eV was ascribed to the lattice oxygen O^{2-}, and the peak at 531.5 eV was assigned to surface adsorbed oxygen, OH groups and oxygen vacancies. The peak at 532.9 eV was due to chemically or physically adsorbed water and that at 533.6 eV likely to

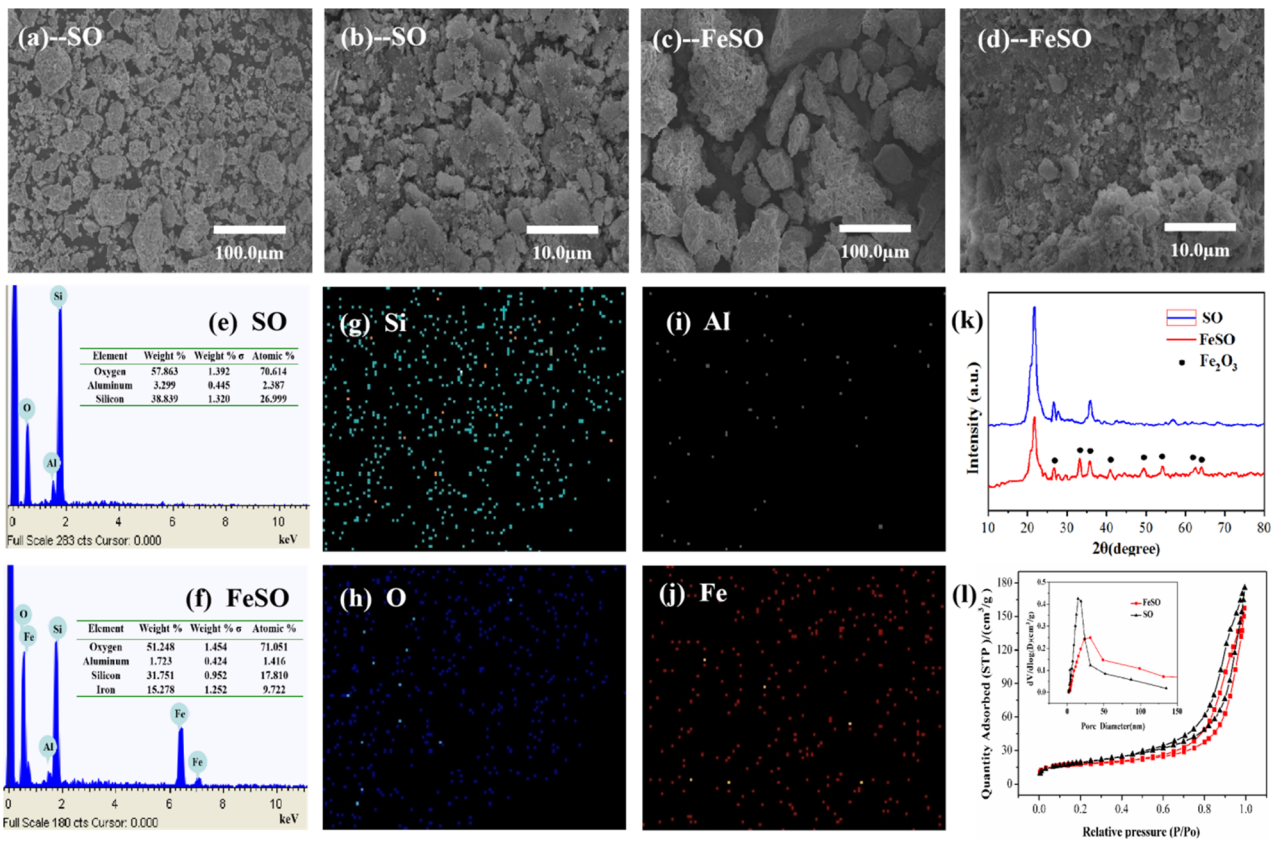

Fig. 1 (a–d) SEM images of SO and FeSO. (e and f) EDS spectrum of SO, FeSO, and (g–j) EDS mapping images of FeSO. (k) XRD of SO and FeSO. (l) N_2 adsorption–desorption isotherms and pore size distribution of SO and FeSO.

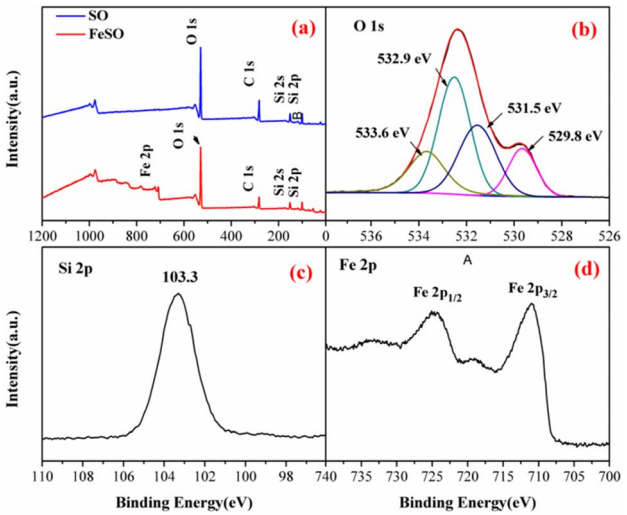

Fig. 2 (a) XPS spectra analysis of SO and FeSO, (b) O 1s, (c) Si 2p, and (d) Fe 2p of the FeSO composites.

be associated with Si–O–Si.[29,30] The OH groups and oxygen vacancies play an important role in the higher activity of the catalyst.[31,32] Fig. 2c showed the peak at 103.3 eV was corresponding to Si–O–Si.[33]

The peaks at 711, 718.5, and 724.1 eV represented the binding energies of Fe $2p_{3/2}$, shake-up satellite Fe $2p_{3/2}$, and Fe $2p_{1/2}$, respectively.[34] The energy separation between Fe $2p_{3/2}$ and Fe $2p_{1/2}$ was more than 13 eV, indicating the existence of Fe^{3+}.[35] In addition, the surface Fe concentration was 25.7 wt% by the data of XPS measurement.

Fig. S1† shown the FTIR spectra of the SO and FeSO. From this figure, the Si–O bonds appeared at the peaks of 1105 cm^{-1}.[36] The band observed at 1635 cm^{-1} correspond to –OH stretching vibration, which proved the presence of adsorbed water on the surface.[37] The bands observed at 3419 cm^{-1} was corresponding to the typical hydroxyl absorption band.[38]

3.2 Controlled experiment

Fig. 3a and b showed the degradation and mineralization curves of SMX as a function time in $FeSO/O_2$, ozone alone and $FeSO/O_3$. Adsorption experiments were first carried out, and the adsorption process leaded to 14.7% SMX removal in 30 min and 5.9% TOC removal in 60 min. Compared with the catalytic ozonation process, SMX removed by adsorption was not much less. Besides, ozonation alone achieved 35.1% SMX degradation in 30 min and 22.0% mineralization in 60 min. Both SMX degradation and mineralization were enhanced significantly when introducing FeSO into ozonation process, which lead to 88.1% SMX degradation in 30 min and 49.1% mineralization in 60 min. As a whole, the SMX degradation efficiency and TOC removal of $FeSO/O_3$ system were much better than those of $FeSO/O_2$ and ozonation alone systems. It indicated that FeSO particles played a critical role in catalyzing ozone oxidation process for SMX removal.

3.3 Effects of operating parameters of FeSO catalytic ozonation process

3.3.1. Effect of reaction temperature. Under different reaction temperatures from 5 °C to 20 °C, the SMX degradation and TOC removal by ozonation with/without FeSO were studied in Fig. 4a and b. For ozonation alone, the low degradation efficiency of SMX after 30 min were 12.1% at 5 °C, 15.6% at 10 °C, 28.9% at 15 °C and 35.1% at 20 °C, respectively. Ozone alone had the weak oxidation ability for SMX degradation, especially at low temperature, which was in good consistence with previous reports.[39] For catalytic ozonation process, the degradation efficiency increased with the increasing reaction temperature. At different temperatures, catalytic ozonation process always revealed higher degradation rate than ozonation alone. The temperature significantly influenced the SMX degradation in the presence of FeSO. As shown in Fig. 4b, the removal rate of TOC in $FeSO/O_3$ was significantly higher than that in ozonation alone under different temperature conditions. The temperature barely influenced the removal of TOC in $FeSO/O_3$ system, and all the removal rates of TOC were more than 50% within 60 min. The above results again suggested that the FeSO had high catalytic ozonation activity.

3.3.2. Effect of initial solution pH. Fig. 5 showed the effect of the initial pH on SMX degradation and TOC removal by the FeSO catalyzed ozonation system. It can be seen that SMX degradation increased when tuning pH from acidic to alkaline. This increase trend was more noticeable on TOC removal. SMX

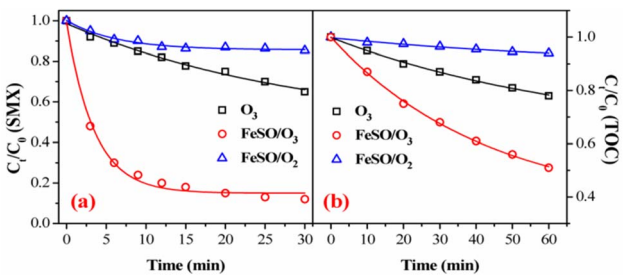

Fig. 3 (a) Degradation and (b) mineralization of SMX among various reaction systems (experiment conditions: $[SMX]_0 = 20$ mg L^{-1}, ozone dosage = 0.4 mg min^{-1}, FeSO = 1.0 g L^{-1}, initial pH = 7.0 and $T = 20 \pm 1$ °C).

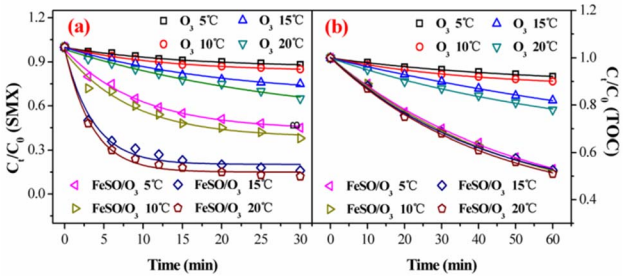

Fig. 4 Effect of reaction temperature on (a) degradation and (b) mineralization of SMX in ozone alone and $FeSO/O_3$ system (experiment conditions: $[SMX]_0 = 20$ mg L^{-1}, ozone dosage = 0.4 mg min^{-1}, FeSO = 1.0 g L^{-1} and initial pH = 7.0).

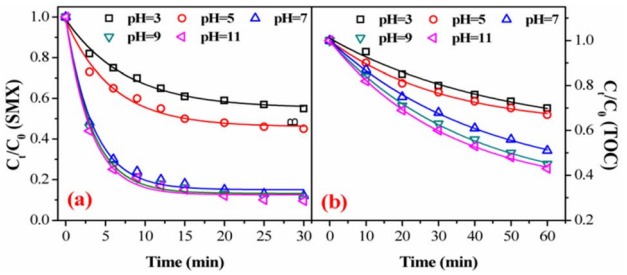

Fig. 5 Effect of initial solution pH value on (a) degradation and (b) mineralization of SMX in FeSO/O_3 (experiment conditions: $[SMX]_0$ = 20 mg L^{-1}, ozone dosage = 0.4 mg min^{-1}, FeSO = 1.0 g L^{-1} and T = 20 ± 1 °C).

degradations achieved only 42.0% at pH 3.0 and 54.8% at pH 5.0, respectively, while it achieved 90.5% at high pH 11.0. This phenomenon can be explained as followed: at low pH of 3, ozone was the main oxidant thus leading to lower SMX degradation. While pH changed from 7 to 11, ˙OH and ozone were the predominant oxidants causing more SMX degradation.[40] Correspondingly, TOC removal increased with increasing the initial pH. Overall, the SMX degradation and TOC removal by FeSO catalyzed ozonation were found to strongly rely on the solution pH value.

3.3.3. Effect of catalyst dosage. Catalyst dosage is another important factor during catalytic ozonation process, which could greatly influence the decomposition rate of ozone for ˙OH generation. The catalytic activity of FeSO with various dosages was evaluated by the degradation and mineralization of SMX at initial pH of 7.0. Ozonation alone without catalyst achieved 35.1% degradation after 30 min and 22.0% mineralization after 60 min, respectively (Fig. 6). In contrast, the addition of FeSO significantly enhanced the SMX degradation and mineralization. With the increase of catalyst dosage from 0.50 g L^{-1} to 1.50 g L^{-1}, the degradation rate of SMX increased from 71.5% to 92.9% and the removal rate of TOC increased from 32.9% to 56.9%. However, when the catalyst dosage was increased from 1.0 g L^{-1} to 1.5 g L^{-1}, the degradation rate and mineralization rate of SMX increased slightly, because of the limited amount of ozone in the system.[34]

3.3.4. Effect of initial concentration. Fig. S2† showed the influence of initial concentration on the degradation and mineralization efficiency of SMX during FeSO/O_3. The results showed that the removal rate of SMX decreased with the increase of initial concentration of solution. This may be because, on the one hand, the degradation and mineralization of SMX mainly depend on the amount of ozone molecules and ˙OH in the solution. Under the same experimental conditions, the amount of dissolved ozone molecules and ˙OH produced in the solution was almost the same. Therefore, the ability to degrade and mineralize SMX was close. With the increase of the initial concentration of the solution, the efficiency of SMX degradation and mineralization gradually declined. On the other hand, with the increase of the initial concentration of the solution, the intermediate products of SMX degradation in the solution also increased, which competed to consume ozone molecules and ˙OH in the solution. Therefore, the degradation rate of SMX and the removal rate of TOC decreased with the increase of initial solution concentration.

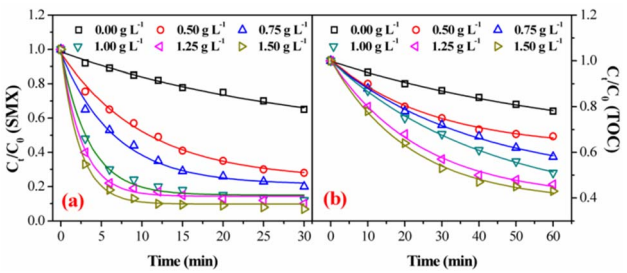

Fig. 6 Effect of catalyst dosage on degradation (a) and mineralization (b) of SMX in FeSO/O_3 (experiment conditions: $[SMX]_0$ = 20 mg L^{-1}, ozone dosage = 0.4 mg min^{-1}, initial pH = 7.0, T = 20 ± 1 °C).

3.3.5. Effect of inorganic anions. The adsorption of some inorganic ions on catalyst surface may affect the catalytic activity of the catalyst.[41] In this study, the effects of general inorganic cations and anions on FeSO catalyzed ozonation were investigated. As shown in Fig. 7a, the common inorganic cations had a slight inhibitory effect on the degradation and mineralization of SMX. The existence of Ca^{2+} and Mg^{2+} reduced the degradation rate of SMX by 5.5% and 5.9% respectively, and the mineralization rate by 4.7% and 4.8% respectively. The reason for this phenomenon may be that these two inorganic cations occupied the catalytic active site of FeSO through the coordination and complexation with the hydroxyl groups of FeSO surface. By contrast, the existence of K^+ and Na^+ had little effect on the degradation and mineralization rate of SMX due to their weak adsorption and complexation ability on the surface of FeSO.

Among these common anions, PO_4^{3-} has the greatest impact on the ozonation of SMX probably because of the strongest complexation ability. The surface of FeSO catalyst was rich in hydroxyl groups, which can catalyze ozone to produce ˙OH. When PO_4^{3-}, SO_4^{2-} and Cl^- were added, the hydroxyl groups on the catalyst surface were replaced or complexed by these ions, which reduced available amount of hydroxyl groups and subsequently the catalytic activity. In addition, some research results showed that the metal ions could be used as Lewis acid, and it would be inactivated by occupying the hydroxyl group active site (eqn (1) and (2)).[42] In the presence of 50 mg L^{-1} phosphate, the degradation rate of SMX decreased significantly. It suggested that most of the active sites on the surface of FeSO catalyst were occupied by phosphate, which negatively affected its ability of catalyze ozonation.

$$\cdot OH + H_2PO_4^- \rightarrow HO^- + H_2PO_4,\ k < 105\ M^{-1}\ s^{-1} \quad (1)$$

$$\cdot OH + HPO_4^{2-} \rightarrow HO^- + HPO^-,\ k < 107\ M^{-1}\ s^{-1} \quad (2)$$

3.4 Catalyst stability and re-use potential

In order to investigate the stability of the catalyst, five cycle experiments were carried out under the same experimental

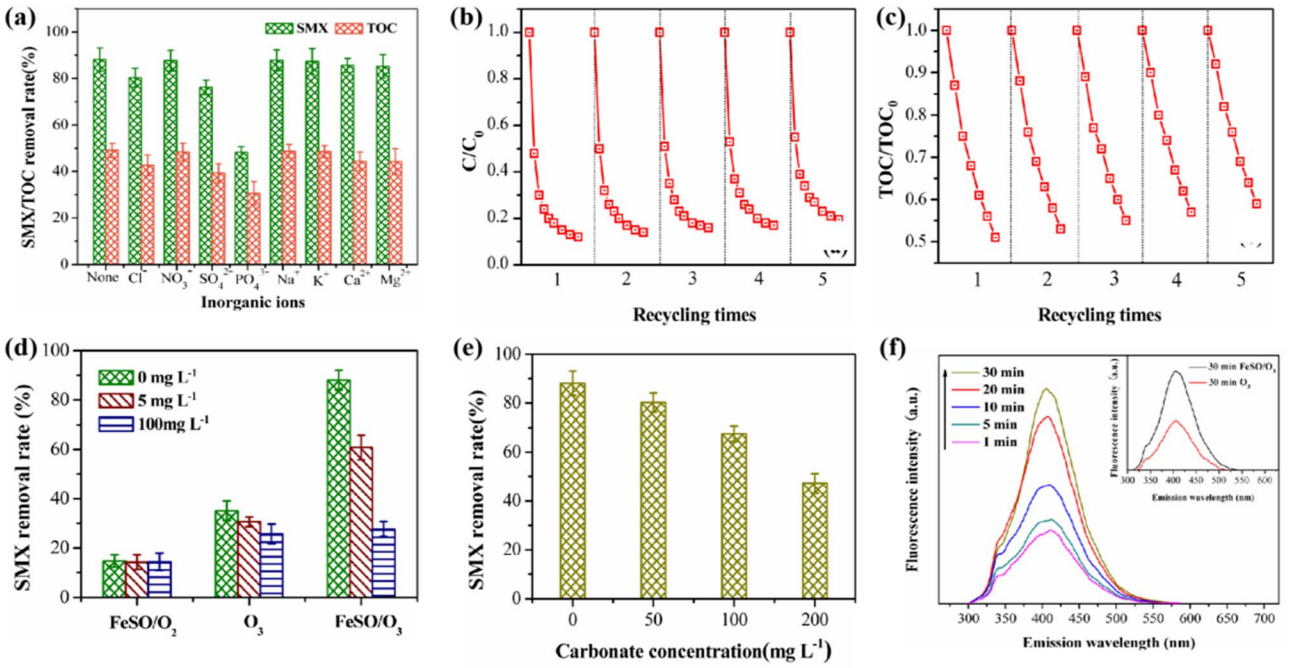

Fig. 7 (a) Effect of inorganic ions on SMX removal. (b and c) Effect of recycling times on SMX degradation and mineralization. (d) Effect of TBA on SMX degradation with and without FeSO. (e) Effect of HCO_3^- on SMX degradation. (f) Influence of irradiation time on fluorescence spectrum in FeSO/O_3 process.

conditions. After each experiment, FeSO was cleaned, filtered and dried. As shown in Fig. 7b and c, the degradation and mineralization effects of SMX decreased slightly, and the degradation rates of SMX were 88.1%, 85.7%, 83.2%, 81.7% and 80.5% respectively for the five cycles of experiments. The TOC removal rate decreased from 49.1% to 40.5%. After five times of reuse, the degradation and mineralization effect of FeSO catalytic ozonation system on SMX declined to a small extent, and the catalyst still maintained high catalytic activity. It indicated that FeSO catalyst had good reusability and stability. In addition, the dissolution of iron ions in continuous FeSO catalyzed ozonation reaction system was studied in Table S4.† After repeated experiments, the dissolution concentration of iron ions was less than the national limit concentration of 0.3 mg L^{-1}, and met China's hygienic standard for drinking water (GB5749-2006).

3.5 Possible reaction mechanisms

3.5.1 ˙OH identification. TBA (5 mg L^{-1} and 100 mg L^{-1}) was used as free radical scavenger in the experiment.[24] As illustrated in Fig. 7d, the addition of TBA did not affect the adsorption of FeSO catalyst on SMX. Under the condition of ozone oxidation alone, the addition of TBA slightly decreased the degradation rate of SMX, indicating that ozone was hard to decompose to produce ˙OH without catalyst. Whereas, SMX was still degraded by 25.7% mainly due to the synergistic effect of ozone direct oxidation and catalyst adsorption. In the FeSO/O_3 catalytic ozonation system, the addition of 5 mg L^{-1} TBA greatly inhibited the degradation of SMX, while the inhibition enhanced as 100 mg L^{-1} TBA was added. The reason for this phenomenon is that TBA competed with pollutants to consume ˙OH and therefore inhibited the oxidative degradation of SMX by ˙OH.

The experiment of the addition of HCO_3^- further confirmed our conclusion. HCO_3^- was an another well-known ˙OH capture agent in catalytic ozonation reaction systems. When the pH of the solution was 7, HCO_3^- mainly exists in the solution, and its reaction rate constant with ˙OH was 1.5 × 107 M^{-1} s^{-1}.[43] As shown in Fig. 7e, when the pH of the aqueous solution was 7, HCO_3^- had a certain inhibitory effect on the degradation of SMX. With the increase of HCO_3^- in the solution, the inhibition effect on the degradation of SMX became obvious. Excessive HCO_3^- can lead to rapid consumption of ˙OH. In the process of heterogeneous catalytic ozonation degradation of SMX, HCO_3^- and CO_3^{2-} will compete with SMX to participate in free radical reactions, consuming a large amount of ˙OH, thereby reducing the removal effect of SMX. It can be inferred that the process of FeSO catalyzed ozonation of SMX may follow the oxidation mechanism of ˙OH.

Subsequently, the amount of ˙OH in the different reaction time was analyzed by photoluminescence (PL) spectrum. Hydroxybenzoic acid was generated by using benzoic acid as ˙OH capture agent. The change of its strength can indirectly reflect the amount of ˙OH generated. As shown in Fig. 7f, the fluorescence of the products intensified gradually with the extension of catalytic ozonation time in the FeSO catalytic ozonation system. The amount of ˙OH gradually increased with the extension of reaction time. When the reaction proceeded to 30 min, the amount of ˙OH generated in FeSO/O_3 system was the most, significantly higher than that in single ozonation system for 30 min.

3.5.2. Reaction mechanism. The FT-IR characterization results of FeSO showed that the catalyst surface was rich in surface hydroxyl groups (Fig. S1†). The peak splitting resulted of O 1s in XPS of FeSO catalyst showed that the surface oxygen was mainly from hydroxyl groups (Fig. 2). The hydroxyl groups in the catalyst played a very important role in catalytic ozonation that directly affected the catalytic activity. Based on the chain reaction of ozone decomposition on the catalyst surface (eqn (3)–(7)), the generated ·OH could react quickly with organic pollutants adsorbed on the FeSO surface and in the aqueous solution, thus improving the degradation and mineralization effect of the reaction solution.[44]

$$O_3 + H_2O \rightarrow 2{\cdot}OH + O_2,\ k_2 = 1.1 \times 10^{-4}\ M^{-1}\ s^{-1} \quad (3)$$

$$O_3 + OH^- \rightarrow O_2{\cdot}^- + HO_2{\cdot},\ k_2 = 70\ M^{-1}\ s^{-1} \quad (4)$$

$$O_3 + {\cdot}OH \rightarrow O_2 + HO_2{\cdot} \leftrightarrow O_2{\cdot}^- + H^+ \quad (5)$$

$$O_3 + HO_2{\cdot} \rightarrow 2O_2 + {\cdot}OH,\ k_2 = 1.6 \times 10^{9}\ M^{-1}\ s^{-1} \quad (6)$$

$$2HO_2{\cdot} \rightarrow O_2 + H_2O_2 \quad (7)$$

There may be three pathways in the process of FeSO catalyzed ozonation of SMX in this study, as shown in Fig. 8: (a) ozone and organic molecules were simultaneously adsorbed on the surface of FeSO catalyst, resulting in direct oxidation reaction. (b) When FeSO was put into aqueous solution, a dense layer of surface hydroxyl was formed on its surface. It would promote the decomposition of ozone molecules adsorbed on the catalyst surface into ·OH, which can rapidly oxidize SMX and its intermediates. (c) The organic molecules adsorbed on the catalyst surface, and then they can be oxidized by ozone molecules and ·OH in aqueous solution.

3.6 Products identification and proposed degradation pathways

The mineralization of SMX was measured under various systems. Although the removal efficiency of TOC in the constructed system was 49.1%, and adsorption removal (5.9%), suggesting that SMX was mostly degraded into small molecule intermediates rather than complete mineralization.[45] To gain an insight into the degradation behavior of SMX, LC-MS technologies were employed to analyze the reaction solution.

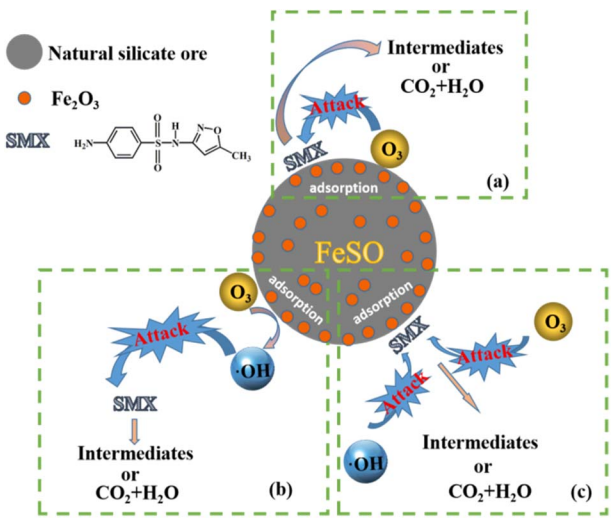

Fig. 8 Reaction mechanism of the FeSO process.

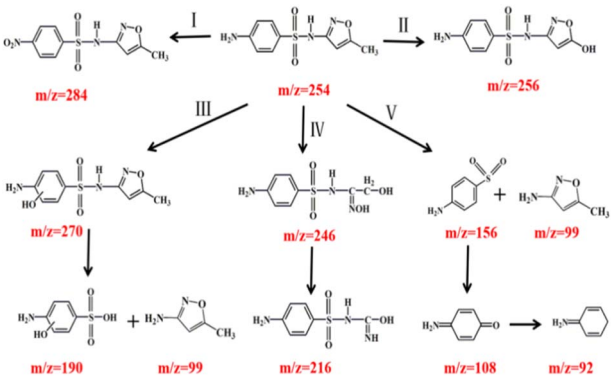

Fig. 9 Proposed degradation pathways of SMX.

During the catalytic ozonation process, numerous reaction intermediates may be formed due to the non-selective nature of ·OH.[46] Analytic results of degradation products in SMX were shown in Fig. S3† and summarized in Table S5.† Ten kinds of main intermediates $[M + H]^+$ peaked at m/z 99, 156, 190, 246, 256, 270, 284, 108, 92 and 216 were detected by LC-MS, respectively.

Possible degradation pathways of SMX were proposed in Fig. 9. In pathway I, reactive site N of SMX was attacked by ·OH and formed DP7 ($m/z = 284$). In pathway II, intermediate DP5 ($m/z = 256$) mass units could be attributed to the substitution of the methyl group by ·OH attacking on the isoxazole ring, resulting in the formation of hydroxylated structure.[47] In pathway III, electrophilic replacement on C of the aromatic ring by ·OH formed DP6 ($m/z = 270$) as the ortho-hydroxylated SMX. Then ·OH attacking on S–N bond of phenylcyclic amide resulted in the generation of DP1 ($m/z = 99$) and DP3 ($m/z = 190$).[48] In pathway IV, the isoxazole ring was cleaved to produce DP4 ($m/z = 246$). The dehydrogenation reaction on alcohol group and the loss of one carbonyl group formed the intermediate DP10 ($m/z = 216$). In pathway V, the cleavage of S–N bond resulting from the ·OH attack on the sulfonamide bond generated DP2 ($m/z = 156$) and DP1 ($m/z = 99$). The reason for bond breakage was the S atom in sulfonamide group was easily attacked by reactive oxygen species.[49] Meanwhile, ·OH attacked DP2 and resulted in the generation of DP8 ($m/z = 108$) and DP9 ($m/z = 92$).[50]

4. Conclusions

In this work, natural silicate ore supported Fe_2O_3 (FeSO) was successfully synthesized for catalytic ozonation of sulfamethoxazole (SMX). The degradation and mineralization effects of SMX by FeSO adsorption, ozonation alone and FeSO/O_3 systems were compared in detail. Due to the addition of FeSO catalyst, the efficiency of ozonation of SMX was significantly improved, which was 53% higher than that of ozonation of SMX alone. The

degradation and mineralization efficiency of SMX increased with the increase of catalyst dosage, initial solution pH and reaction temperature. FeSO catalyst showed the good stability, and the degradation rate of SMX and TOC removal rate slightly decreased after five cycles of experiments. The possible reaction mechanism for the ozone oxidation catalyzed by FeSO was proposed, and the main degradation products for SMX were detected and the corresponding degradation pathways were then speculated.

Conflicts of interest

There are no conflicts to declare.

Acknowledgements

This work was supported by National Natural Science Foundation of China (Grant No.51908162), Open Project of State Key Laboratory of Urban Water Resource and Environment, Harbin Institute of Technology (No. QAK202109), Science Foundation of Heilongjiang Province (Grant No. LH2020E053) and Major science and technology projects of Jilin Institute of Chemical Technology (Grant NO. 2018027).

References

1 X. H. Liu, H. P. Li, Y. Fang, *et al.*, *Sep. Purif. Technol.*, 2021, **274**, 118945.
2 A. Mirzaei, L. Yerushalmi, Z. Chen, *et al.*, *J. Hazard. Mater.*, 2018, **359**, 516.
3 S. Gao, Z. Zhao, Y. Xu, *et al.*, *J. Hazard. Mater.*, 2014, **274**, 258–269.
4 S. Babić, M. Zrnčić, D. Ljubas, *et al.*, *Environ. Sci. Pollut. Res.*, 2015, **22**, 11372.
5 S. Ding, J. Niu, Y. Bao and L. Hu, *J. Hazard. Mater.*, 2013, **262**, 812.
6 Y. Lin, C. Yang, Q. Niu, *et al.*, *Adv. Funct. Mater.*, 2022, **32**, 2108814.
7 L. Luo, D. Zou, D. Lu, *et al.*, *RSC Adv.*, 2018, **58**, 33534.
8 A. B. Thomsen and H. H. Kilen, *Water Res.*, 1998, **32**, 3353.
9 C. Wang, K. Ma, T. Wu, M. Ye and P. K. Tan, *Chemosphere*, 2016, **149**, 219.
10 S. Zha, Y. Cheng, Y. Gao, *et al.*, *Chem. Eng. J.*, 2014, **255**, 141.
11 Z. Heidari, R. Pelalak, R. E. Malekshah, *et al.*, *Chem. Eng. J.*, 2022, **428**, 131230.
12 J. L. Wang and Z. Y. Bai, *Chem. Eng. J.*, 2017, **312**, 79.
13 Z. Q. Liu, J. Tu, Q. Wang, *et al.*, *Sep. Purif. Technol.*, 2018, **200**, 51.
14 H. M. Jalali, *Mater. Sci. Eng., C*, 2016, **50**, 924.
15 B. Y. Lan, R. H. Huang, L. S. Li, H. H. Yan, G. Z. Liao, X. Wang and Q. Y. Zhang, *Chem. Eng. J.*, 2013, **219**, 346.
16 D. Yu, M. Wu, Q. Hu, L. Wang, C. Lv and L. Zhang, *J. Hazard. Mater.*, 2019, **367**, 456.
17 D. Wang, H. Xu, J. Ma, *et al.*, *Water Res.*, 2019, **149**, 136.
18 J. Wang and Z. Bai, *Chem. Eng. J.*, 2016, **312**, 79.
19 J. Ma, M. Sui, T. Zhang and C. Guan, *Water Res.*, 2005, **39**, 779.
20 Y. Xie, S. Peng, Y. Feng and D. Wu, *Chemosphere*, 2020, **239**, 124612.
21 D. Gümüş and F. Akbal, *Chemosphere*, 2017, **174**, 218.
22 X. Yang, X. Cheng, A. A. Elzatahry, *et al.*, *Chin. Chem. Lett.*, 2019, **2**, 324.
23 D. Wang, H. Xu, J. Ma, *et al.*, *Chem. Eng. J.*, 2018, **354**, 113.
24 G. Moussavi, R. Khosravi and N. R. Omran, *Appl. Catal., A*, 2012, **445**, 42.
25 K. He, Y. Dong, L. Yin, A. Zhang and Z. Li, *Acta Geochim.*, 2006, **159**, 587.
26 H. Xiong, D. Zou, D. Zhou, *et al.*, *Chem. Eng. J.*, 2017, **316**, 7.
27 J. Bing, C. Hu, Y. Nie, *et al.*, *Environ. Sci. Technol.*, 2015, **49**, 1690.
28 J. Lu, X. Wei, Y. Chang, *et al.*, *J. Chem. Technol. Biotechnol.*, 2015, **91**, 985.
29 Y. Ren, H. Zhang, H. An, *et al.*, *J. Colloid Interface Sci.*, 2018, **526**, 347.
30 Y. Huang, W. Xu, L. Hu, *et al.*, *Catal. Today*, 2017, **297**, 143.
31 M. A. Peluso, L. A. Gambaro, E. Pronsato, *et al.*, *Catal. Today*, 2008, **133**, 487.
32 H. Chen, A. Sayari, A. Adnot, *et al.*, *Appl. Catal., B*, 2001, **32**, 195.
33 B. M. Reddy, B. Chowdhury and P. G. Smirniotis, *Appl. Catal., A*, 2001, **221**, 397.
34 H. Xiong, S. Dong, J. Zhang, *et al.*, *Water Res.*, 2018, **136**, 75.
35 W. J. Liu, F. Zeng, H. Jiang, X. S. Zhang and W. W. Li, *Chem. Eng. J.*, 2012, **180**, 9.
36 Q. Fei, B. Xu, Z. Lun, *et al.*, *Appl. Catal., B*, 2012, **121**, 171.
37 F. Z. Zhang, C. H. Wei, *et al.*, *Appl. Catal., A*, 2017, **547**, 60.
38 L. Qi, H. You, Z. Zhang, *et al.*, *Int. J. Electrochem. Sci.*, 2013, **8**, 5457.
39 D. Wang, H. Xu, J. Ma, *et al.*, *Water Res.*, 2019, **149**, 136.
40 Z. K. Xiong, B. Lai, Y. Yuan, J. Y. Cao, P. Yang and Y. X. Zhou, *Chem. Eng. J.*, 2016, **302**, 137.
41 J. Nawrocki and B. Kasprzyk-Hordern, *Appl. Catal., B*, 2010, **99**, 27.
42 W. J. Masschelein, *Environ. Sci. Pollut. Res.*, 1992, **1**, 13.
43 W. Li, Z. Qiang, T. Zhang, *et al.*, *Appl. Catal., B*, 2012, **113**, 290.
44 R. Huang, H. Yan, L. Li, D. Deng, Y. Shu and Q. Zhang, *Appl. Catal., B*, 2011, **106**, 264.
45 S. Wu, C. Yang, Y. Lin, *et al.*, *J. Environ. Sci.*, 2022, **115**, 330–340.
46 W. Q. Guo, R. L. Yin, X. J. Zhou, J. S. Du, H. O. Cao, S. S. Yang, *et al.*, *Ultrason. Sonochem.*, 2015, **22**, 182.
47 A. M. Wang, Y. Y. Li and A. L. Estrada, *Appl. Catal., B*, 2011, **102**, 378.
48 J. S. Du, W. Q. Guo, H. Z. Wang, *et al.*, *Water Res.*, 2018, **138**, 323–332.
49 X. Fu, Y. Lin, C. Yang, *et al.*, *J. Environ. Eng.*, 2022, **10**, 107734.
50 A. G. Trovo, R. F. Nogueira, A. Aguera, *et al.*, *Water Res.*, 2009, **43**, 3922.